Sensorless Sliding-Mode Control of Induction Motors

Zhang Yan, Changxi Jin, and Vadim I. Utkin, *Senior Member, IEEE*

***Abstract*—This paper develops the ideas of speed- and flux-sensorless sliding-mode control for an induction motor illustrated in previous work by one of the authors. A sliding-mode observer/controller is proposed in this paper. The convergence of the nonlinear time-varying observer along with the asymptotic stability of the controller is analyzed. Pulsewidth modulation implementation using sliding-mode concepts is also discussed. The major attention is paid to torque control, and then the developed approach is utilized for speed control. Computer simulations and experiments have been carried out to test the proposed estimation and control algorithm. The experimental results demonstrated high efficiency of the proposed estimation and control method.**

***Index Terms*—Induction motor drives, observers, sliding-mode control, torque and speed control.**

I. Introduction

SENSORLESS control of induction motor (IM) drives is now receiving wide attention [1]. The main reason is that the speed sensor spoils the ruggedness and simplicity of IMs. In a hostile environment, speed sensors cannot even be mounted. However, due to the high order and nonlinearity of the dynamics of an IM, estimation of the angle speed and rotor flux without the measurement of mechanical variables becomes a challenging problem. To overcome these difficulties, various control algorithms have been devised in the literature. Bose *et al.* [2] proposed a hybrid vector control where indirect vector control (IVC) mode at zero-speed transitions to direct vector control (DVC) at high speed, and then transitions back to IVC at zero speed. Kubota *et al.* [3] suggested a speed adaptive flux observer with an adaptive compensator for the variation of the rotor resistance. Based on the model reference adaptive control theory, a speed estimator with pole placement in [4] was developed. Tajima *et al.* [5] proposed speed estimation by the output difference of the current model and voltage model. Dixon *et al.* [6] developed a speed and position estimator based on the introduction of a constant-frequency carrier signal in the stator currents. Kim *et al.* [7] proposed a novel estimation strategy for the very-low-speed operation to estimate both the instantaneous speed and disturbance load torque using Kalman filter.

Sliding-mode control theory, due to its order reduction, disturbance rejection, strong robustness, and simple implementation by means of power converter, is one of the prospective control methodologies for electrical machines.The basic concepts and principles of sliding-mode control of electric drives were demonstrated in [1] and some aspects of the implementation are illustrated in [8]. Zaremba [9] suggested a sliding-mode speed observer in d–q coordinate with stability and robustness analysis for the system with constant speed.

In this paper, we propose a closed-loop speed and flux estimator based on the sliding-mode control methodology. Applying the estimator, the corresponding sliding-mode torque controller is designed. Then, it is shown that speed control can be achieved by using the torque controller. The conditions of the asymptotic stability of the sliding-mode control system and the convergence of the sliding-mode observer are also discussed. The efficiency of estimator and controller is shown by both simulation and experiments.

Manuscript received January 19, 2000; revised August 10, 2000. Abstract published on the Internet September 6, 2000.

Z. Yan and V. I. Utkin are with the Department of Electrical Engineering, The Ohio State University, Columbus, OH 43210 USA.

C. Jin is with Fujitsu USA, Santa Clara, CA 95050 USA.

Publisher Item Identifier S 0278-0046(00)10265-5.

II. Dynamic Model of IM and Problem Statement

A. Dynamic Model of IM

Under the commonly used assumptions, equations for an IM in the orthogonal stator frame [(α, β) coordinate] can be expressed as [12]

$$\frac{dn}{dt} = \frac{P}{J}(M - M_L) \tag{1}$$

$$M = \frac{3P}{2}\frac{x_H}{x_R}(i_\beta\phi_\alpha - i_\alpha\phi_\beta) \tag{2}$$

$$\frac{d\phi_\alpha}{dt} = -\eta\phi_\alpha - n\phi_\beta + \eta x_H i_\alpha \tag{3}$$

$$\frac{d\phi_\beta}{dt} = -\eta\phi_\beta + n\phi_\alpha + \eta x_H i_\beta \tag{4}$$

$$\frac{di_\alpha}{dt} = \beta\eta\phi_\alpha + \beta n\phi_\beta - \gamma i_\alpha + \frac{1}{\sigma x_S}u_\alpha \tag{5}$$

$$\frac{di_\beta}{dt} = \beta\eta\phi_\beta - \beta n\phi_\alpha - \gamma i_\beta + \frac{1}{\sigma x_S}u_\beta \tag{6}$$

with stator voltage and current vector defined as

$$\begin{bmatrix} u_\alpha \\ u_\beta \end{bmatrix} = \frac{2}{3}\begin{bmatrix} e_{R\alpha} & e_{S\alpha} & e_{T\alpha} \\ e_{R\beta} & e_{S\beta} & e_{T\beta} \end{bmatrix}\begin{bmatrix} u_R \\ u_S \\ u_T \end{bmatrix} \tag{7}$$

$$\begin{bmatrix} i_\alpha \\ i_\beta \end{bmatrix} = \frac{2}{3}\begin{bmatrix} e_{R\alpha} & e_{S\alpha} & e_{T\alpha} \\ e_{R\beta} & e_{S\beta} & e_{T\beta} \end{bmatrix}\begin{bmatrix} i_R \\ i_S \\ i_T \end{bmatrix} \tag{8}$$

where n is the electrical rotor angle velocity; two-dimensional vectors $\phi^T = (\phi_\alpha, \phi_\beta)$, $i^T = (i_\alpha, i_\beta)$, and $u^T = (u_\alpha, u_\beta)$ are rotor flux, stator current, and voltage in (α, β) coordinate, respectively; M and M_L are the torque developed by the motor and the load torque; J is inertia of the rotor; P is the number of pole pairs; and $(u_R, u_S, u_T)^T$ and $(i_R, i_S, i_T)^T$ are phase

0278–0046/00$10.00 © 2000 IEEE

voltage and current respectively. e_R, e_S, e_T are unit vectors of the three-phase windings R, S, T.

η, β, σ, and γ are positive constants defined as $\eta = (r_R/x_R)$, $\sigma = 1 - (x_H^2/x_S x_R)$, $\beta = (x_H/\sigma x_S x_R)$, and $\gamma = (1/\sigma x_S)(r_S + (x_H^2/x_R^2) r_R)$, where r_R and r_S are rotor and stator resistances, x_R and x_S are rotor and stator inductances, and x_H is the mutual inductance.

B. Control Objective

It is known that the rotor flux is needed for the implementation of torque or speed control. Unfortunately, the rotor flux cannot be measured directly. If the angle speed is available, the flux can be estimated with a second-order observer and its convergence is guaranteed for any speed [1]. However, if no information about the mechanical variables is acquired, the design of the observer is no more a trivial problem. Our objective in this paper is to design a torque or speed tracking controller for the IM given by (1)–(6) without measurement of mechanical variables. Therefore, we have the following problem statement: design a flux/speed observer to estimate the flux and speed simultaneously based on the measurement of the stator currents and voltages, and then design a corresponding controller to guarantee that the real torque or speed tracks the desired torque or speed.

Here, we suggest a nonlinear observer/controller with the following basic ideas. First, in the framework of the approach offered in [10], we design a flux and current observer with discontinuous parameters and stator currents and voltages as its inputs such that the estimated currents converge to the real currents. Then, an ideal sliding-mode controller for flux/torque is designed for estimated values of the flux and speed. The stability analysis of the observer/controller shows that the real flux converges to the estimated flux and the average value of the discontinuous parameter of the observer is equal to the real speed.

III. Sliding-Mode Flux/Speed Observer

Applying the same structure of (3)–(6), the sliding-mode rotor flux, stator current and speed observer is proposed as

$$\frac{d\hat{\phi}_\alpha}{dt} = -\eta\hat{\phi}_\alpha - \hat{n}\hat{\phi}_\beta + \eta x_H i_\alpha + C\hat{\phi}_\beta\mu \tag{9}$$

$$\frac{d\hat{\phi}_\beta}{dt} = -\eta\hat{\phi}_\beta + \hat{n}\hat{\phi}_\alpha + \eta x_H i_\beta - C\hat{\phi}_\alpha\mu \tag{10}$$

$$\frac{d\hat{i}_\alpha}{dt} = \beta\eta\hat{\phi}_\alpha + \beta\hat{n}\hat{\phi}_\beta - \gamma i_\alpha + \frac{1}{\sigma x_S}u_\alpha - \beta\hat{\phi}_\alpha\mu \tag{11}$$

$$\frac{d\hat{i}_\beta}{dt} = \beta\eta\hat{\phi}_\beta - \beta\hat{n}\hat{\phi}_\alpha - \gamma i_\beta + \frac{1}{\sigma x_S}u_\beta - \beta\hat{\phi}_\beta\mu \tag{12}$$

where continuous time function $\hat{\phi}_\alpha$, $\hat{\phi}_\beta$ represent the estimated rotor flux and $\hat{i}_\alpha$, $\hat{i}_\beta$ represent the estimated stator currents. C is a parameter to be selected. The estimate of the angle speed $\hat{n}$ and the auxiliary variable μ are discontinuous parameters given by

$$\hat{n} = n_0 \operatorname{sign} s_n \quad \mu = \mu_0 \operatorname{sign} s_\mu, \qquad n_0,\ \mu_0 \text{ are constants}$$

where s_n and s_μ are nonlinear functions of the stator current errors and estimated rotor flux $s_n = (\hat{i}_\beta - i_\beta)\hat{\phi}_\alpha - (\hat{i}_\alpha - i_\alpha)\hat{\phi}_\beta$, $s_\mu = (\hat{i}_\alpha - i_\alpha)\hat{\phi}_\alpha + (\hat{i}_\beta - i_\beta)\hat{\phi}_\beta$. The method of selecting s_n and s_μ is nothing but the conventional approach to control design based on equation in the frame rotating with rotor flux [13]. It enables one to decouple the design problem of making the estimates $\hat{i}_\alpha$ and $\hat{i}_\beta$ track i_α and i_β into two independent ones.

First, it will be shown that there exist constant values n_0 and μ_0 such that sliding mode occurs in the surfaces of $s_n = 0$ and $s_\mu = 0$ and, as a result, the estimation errors

$$\bar{i}_\alpha = \hat{i}_\alpha - i_\alpha \quad \bar{i}_\beta = \hat{i}_\beta - i_\beta \tag{13}$$

are equal to zero (see Section IV). Then, a sliding-mode controller will be designed (Section V) and it will be shown that the flux estimation errors

$$\overline{\phi}_\alpha = \hat{\phi}_\alpha - \phi_\alpha \quad \overline{\phi}_\beta = \hat{\phi}_\beta - \phi_\beta \tag{14}$$

will tend to zero and the average value of the discontinuous function $\hat{n}$ tends to the real speed n.

IV. Analysis of Current Tracking

To analyze convergence of the estimates to the real values for the proposed observer structure, we first need to analyze the stator current-tracking property. As follows from (3)–(6) and (9)–(12), the sliding-mode observer equations with respect to the errors $\bar{i}_\alpha$, $\bar{i}_\beta$, $\overline{\phi}_\alpha$, and $\overline{\phi}_\beta$ can be written as

$$\frac{d\overline{\phi}_\alpha}{dt} = -\eta\overline{\phi}_\alpha - n\overline{\phi}_\beta - \overline{n}\hat{\phi}_\beta + C\hat{\phi}_\beta\mu \tag{15}$$

$$\frac{d\overline{\phi}_\beta}{dt} = -\eta\overline{\phi}_\beta + n\overline{\phi}_\alpha + \overline{n}\hat{\phi}_\alpha - C\hat{\phi}_\alpha\mu \tag{16}$$

$$\frac{d\bar{i}_\alpha}{dt} = \beta\eta\overline{\phi}_\alpha + \beta n\overline{\phi}_\beta + \beta\overline{n}\hat{\phi}_\beta - \beta\hat{\phi}_\alpha\mu \tag{17}$$

$$\frac{d\bar{i}_\beta}{dt} = \beta\eta\overline{\phi}_\beta - \beta n\overline{\phi}_\alpha - \beta\overline{n}\hat{\phi}_\alpha - \beta\hat{\phi}_\beta\mu. \tag{18}$$

Combining (9), (10), (17), and (18) yields

$$\dot{s}_n = \dot{\bar{i}}_\beta\hat{\phi}_\alpha - \dot{\bar{i}}_\alpha\hat{\phi}_\beta + \bar{i}_\beta\dot{\hat{\phi}}_\alpha - \bar{i}_\alpha\dot{\hat{\phi}}_\beta \tag{19}$$

$$\dot{\bar{i}}_\beta\hat{\phi}_\alpha - \dot{\bar{i}}_\alpha\hat{\phi}_\beta = -\beta\hat{n}\|\hat{\phi}\|^2 + \beta n\|\hat{\phi}\|^2 + \beta\eta e_2 - \beta n e_1 \tag{20}$$

$$\bar{i}_\beta\dot{\hat{\phi}}_\alpha - \bar{i}_\alpha\dot{\hat{\phi}}_\beta = -\hat{n}s_\mu + \eta x_H(\bar{i}_\beta i_\alpha - \bar{i}_\alpha i_\beta) + Cs_\mu\mu. \tag{21}$$

Then,

$$\dot{s}_n = -(\beta\|\hat{\phi}\|^2 + s_\mu)n_0 \operatorname{sign} s_n + f(n, \bar{i}_\alpha, \bar{i}_\beta, e_1, e_2) \tag{22}$$

where $\|\hat{\phi}\| = \sqrt{\hat{\phi}_\alpha^2 + \hat{\phi}_\beta^2}$, $f(n, \bar{i}_\alpha, \bar{i}_\beta, e_1, e_2) = \beta n\|\hat{\phi}\|^2 + \eta x_H(\bar{i}_\beta i_\alpha - \bar{i}_\alpha i_\beta) + \beta\eta e_2 - \beta n e_1 + Cs_\mu\mu$ and

$$e_1 = \overline{\phi}_\alpha\hat{\phi}_\alpha + \overline{\phi}_\beta\hat{\phi}_\beta \tag{23}$$

$$e_2 = \overline{\phi}_\beta\hat{\phi}_\alpha - \overline{\phi}_\alpha\hat{\phi}_\beta. \tag{24}$$

It follows from (22) that, if the condition

$$\beta\|\hat{\phi}\|^2 + s_\mu > 0 \tag{25}$$

TABLE I
PARAMETERS USED IN THE SIMULATION

x_S=590e-6 H	M_L=B*n $N \cdot m$
x_R=590e-6 H	B=0.04 $N \cdot m \cdot s/rad$
x_H=555e-6 H	n_0=120
r_S=0.0106 Ω	μ_0=200
r_R=0.0118 Ω	ϕ_0=0.01
U_0=12.0 V	M_0=1.0 $N \cdot m$
P=1.0	τ=0.0015
J=4.33e-4 $N \cdot m \cdot s^2$	c_2=400

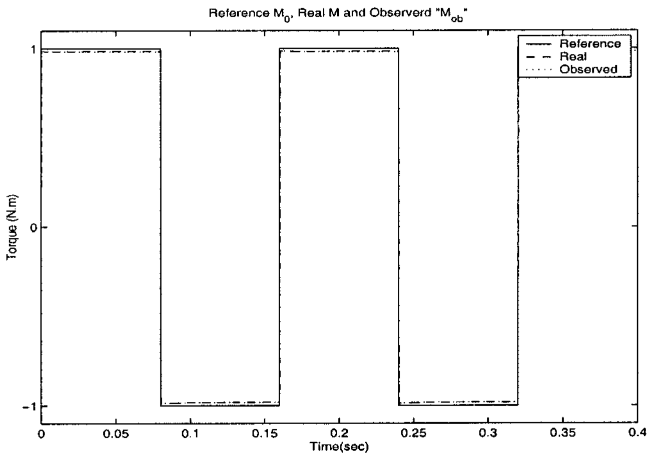

Fig. 1. Torque tracking.

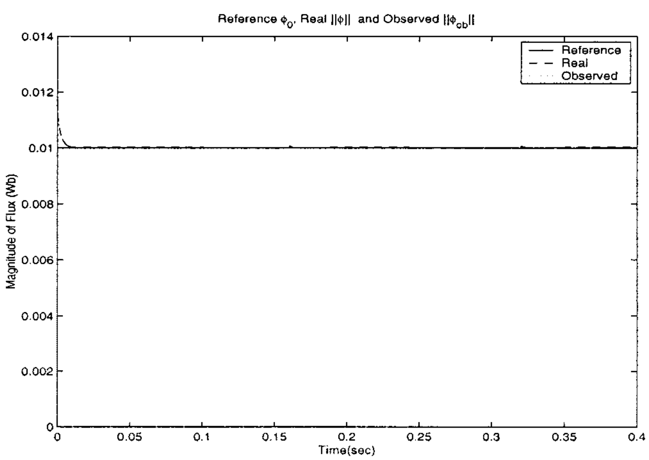

Fig. 2. Magnitude of flux tracking.

holds, then for high enough n_0, $s_n \dot{s}_n < 0$, i.e., sliding mode will occur on surface $s_n = 0$.

Similarly, for s_μ, we have

$$\begin{aligned}\dot{s}_\mu &= \dot{\bar{i}}_\alpha \hat{\phi}_\alpha + \dot{\bar{i}}_\beta \hat{\phi}_\beta + \bar{i}_\alpha \dot{\hat{\phi}}_\alpha + \bar{i}_\beta \dot{\hat{\phi}}_\beta \\ &= \beta\eta e_1 + \beta n e_2 + \eta x_H (i_\alpha \bar{i}_\alpha + i_\beta \bar{i}_\beta) - \beta\mu_0 \|\hat{\phi}\|^2 \mathrm{sign}\, s_\mu. \end{aligned} \tag{26}$$

If μ_0 is high enough, $s_\mu \dot{s}_\mu < 0$, and sliding mode will occur on the surface $s_\mu = 0$.

After sliding mode arises on the intersection of both surfaces $s_n = \bar{i}_\beta \hat{\phi}_\alpha - \bar{i}_\alpha \hat{\phi}_\beta = 0$ and $s_\mu = \bar{i}_\alpha \hat{\phi}_\alpha + \bar{i}_\beta \hat{\phi}_\beta = 0$, then $\bar{i}_\alpha = 0$ and $\bar{i}_\beta = 0$ under the assumption $\|\hat{\phi}\|^2 \neq 0$, which means that the estimated currents $\hat{i}_\alpha, \hat{i}_\beta$ converge to the real currents i_α, i_β.

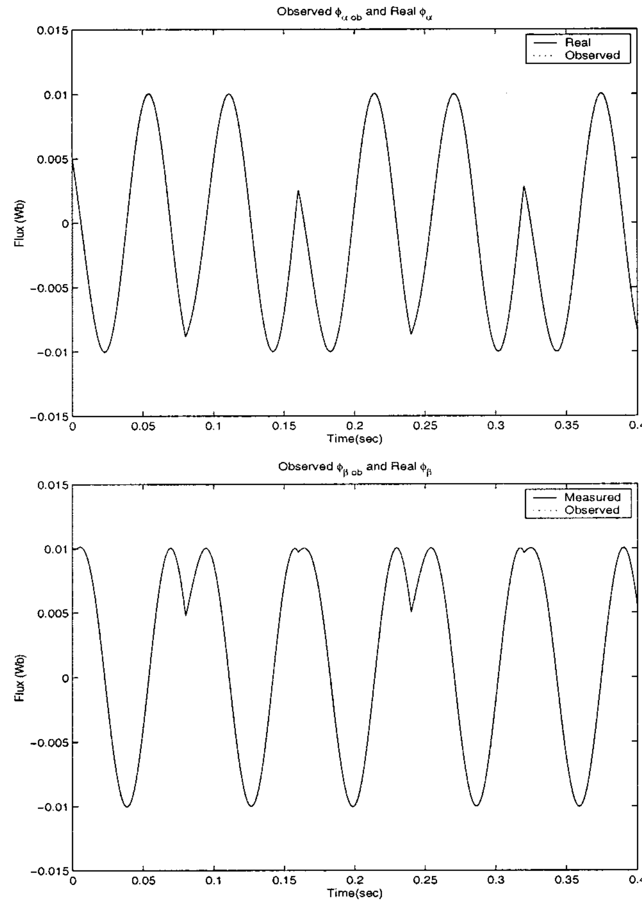

Fig. 3. Flux convergence.

The sliding-mode equations on $s_n = 0$, $s_\mu = 0$ can be derived by replacing the discontinuous functions $n_0 \,\mathrm{sign}\, s_n$ and $\mu_0 \,\mathrm{sign}\, s_\mu$ by the equivalent values n_{eq} and μ_{eq}, which are the solutions of the algebraic equations $\dot{s_n} = 0$ and $\dot{s_\mu} = 0$ [1]. For our case,

$$n_{\mathrm{eq}} = n - \frac{n}{\|\hat{\phi}\|^2} e_1 + \frac{\eta}{\|\hat{\phi}\|^2} e_2. \tag{27}$$

As seen from (27), if the estimated rotor flux converges to the real flux, also, the equivalent rotor speed will tend to the real speed. However, n_{eq} cannot be evaluated by (27), since it contains unknown real rotor flux in the errors e_1 and e_2 [see (23) and (24)]. $\hat{n}$ has slow and high-frequency components, of which the slow component is equal to n_{eq}. Therefore, n_{eq} may be obtained through a low-pass filter [11] with discontinuous value $\hat{n}$ as the input, i.e.,

$$\tau \dot{z} + z = \hat{n}, \qquad z \approx n_{\mathrm{eq}} \tag{28}$$

where τ is the time constant of the low-pass filter. τ should be chosen small enough as compared with the slow component of the real control $\hat{n}$, but large enough to filter out the high rate component [11]. The output z of this low-pass filter is taken as n_{eq}. Since z can be measured directly, in the following analysis we assume that n_{eq} is available.

Remark 1: The condition $\beta\|\hat{\phi}\|^2 + s_\mu > 0$ for sliding mode to occur on the surface $s_n = 0$ is not very restrictive. The reason is that the stator currents i_α and i_β are measurable. We can always choose the initial conditions $\hat{i}_\alpha(0)$ and $\hat{i}_\beta(0)$ close enough to the true stator currents $i_\alpha(0)$ and $i_\beta(0)$ such that the initial errors $\bar{i}_\alpha(0)$ and $\bar{i}_\beta(0)$ or s_μ are small enough to guarantee that the condition (25) holds.

Remark 2: Although the structure of the observer is selected in the framework of [10], modifications are made to guarantee the convergence of the observer. We will show in Section VI that, under certain conditions, the asymptotic stability of the sliding-mode observer can be guaranteed with the flux errors $\bar{\phi}_\alpha$ and $\bar{\phi}_\beta$ converging to zero and z tending to the real speed n.

Remark 3: Although the flux/speed observer is of the fourth order, after sliding mode arises on the surfaces $s_n = 0$ and $s_\mu = 0$, the error equations of the sliding-mode observer are actually of the second order. This order reduction property of the sliding mode is very helpful for the asymptotic stability analysis of the nonlinear time-varying error system.

V. Sliding-Mode Torque Regulation

The control objective in this section is to design a torque tracking controller for the electromechanical system given by (1)–(6). Specifically, based on the rotor flux and speed estimation strategy described in the previous section, we design a corresponding sliding-mode torque controller to guarantee the asymptotic stability of the sliding-mode observer and the torque tracking controller. The additional goal of control dictated by technological requirements is to make the flux track the reference flux input. In this paper, the designs of the observer and the controller are integrated rather than be performed separately.

From the above discussion, three sliding surfaces are designed as

$$s_1 = M_0 - \hat{M} \tag{29}$$

$$s_2 = c_2(\phi_0 - \|\hat{\phi}\|) + \frac{d}{dt}(\phi_0 - \|\hat{\phi}\|) \tag{30}$$

$$s_3 = \int_0^t (u_R + u_S + u_T)\, dt \tag{31}$$

where $\hat{M} = (3P/2)(x_H/x_R)(i_\beta\hat{\phi}_\alpha - i_\alpha\hat{\phi}_\beta)$ is the estimated torque, M_0 and ϕ_0 are the reference torque and the reference magnitude of flux, and c_2 is a positive constant parameter which determines the converge speed of the error $(\phi_0 - \|\hat{\phi}\|)$ in the sliding mode.

In this controller scheme, should sliding mode occur on manifolds $s_1 = 0$ and $s_2 = 0$, the estimated torque and the magnitude of the rotor flux converge to the reference values. Indeed, $s_1 = 0$ means that $M_0 = \hat{M}$ and $s_2 = 0$ means $\phi_0 - \|\hat{\phi}\|$ tends to zero exponentially. In the next section, we will also show that if the estimated flux and torque converge to the reference values, the estimated values will also converge to the real values. Thus, the real flux and torque are forced to the desired value. Manifold s_3 is used just to constitute a three-phase balanced system if all three phase voltages may be selected arbitrarily. Note that this requirement may be redundant.

The design task is reduced to enforcing sliding mode in the manifolds $s = 0$, $s^T = (s_1, s_2, s_3)$ with control $u^T = (u_R, u_S, u_T)$. Equations of the observer/controller motion projection on the subspace $s = (s_1, s_2, s_3)^T$ can be written as

$$\dot{s}_1 = f_1 + a_1(u_\alpha\hat{\phi}_\beta - u_\beta\hat{\phi}_\alpha) \tag{32}$$

$$\dot{s}_2 = f_2 + a_2(u_\alpha\hat{\phi}_\alpha + u_\beta\hat{\phi}_\beta) \tag{33}$$

$$\dot{s}_3 = u_R + u_S + u_T \tag{34}$$

where f_1 and f_2 are continuous state functions,

$$a_1 = \frac{3P}{2}\frac{x_H}{x_S x_R - x_H^2} \quad a_2 = -\frac{1}{\|\hat{\phi}\|}\frac{r_R x_H}{x_S x_R - x_H^2}.$$

Rewriting (32)–(34) in matrix form and taking into account the transformation (7) yield

$$\dot{s} = F + Du \tag{35}$$

where

$$\begin{aligned} F^T &= (f_1,\ f_2,\ 0)\\ u^T &= (u_R,\ u_S,\ u_T)\\ D &= \begin{bmatrix} \frac{2}{3}a_1(e_R \times \hat{\phi}) & \frac{2}{3}a_1(e_S \times \hat{\phi}) & \frac{2}{3}a_1(e_T \times \hat{\phi})\\ \frac{2}{3}a_2(e_R \cdot \hat{\phi}) & \frac{2}{3}a_2(e_S \cdot \hat{\phi}) & \frac{2}{3}a_2(e_T \cdot \hat{\phi})\\ 1 & 1 & 1 \end{bmatrix}\end{aligned}$$

which is nonsingular and $e_i \times \hat{\phi} = e_{i\alpha}\hat{\phi}_\beta - e_{i\beta}\hat{\phi}_\alpha$, $e_i \cdot \hat{\phi} = e_{i\alpha}\hat{\phi}_\alpha + e_{i\beta}\hat{\phi}_\beta$, $i = R, S, T$.

To find the discontinuous controls such that sliding mode is enforced in the manifold $s = 0$, select Lyapunov candidate function $v = (1/2)s^T s \geq 0$. Its time derivative on the state trajectories of system (35)

$$\dot{v} = s^T(F + Du). \tag{36}$$

Following the design methodology introduced in [1], select the discontinuous control

$$u = -U_0 \operatorname{sign} s^*$$

where $s^{*T} = (s_1^*, s_2^*, s_3^*)$, $(\operatorname{sign} s^*)^T = (\operatorname{sign} s_1^*, \operatorname{sign} s_2^*, \operatorname{sign} s_3^*)$, $s^* = D^T s$ and U_0 is a positive constant. Then, (36) can be rewritten as

$$\dot{v} = (s_1^* f_1^* - U_0|s_1^*|) + (s_2^* f_2^* - U_0|s_2^*|) + (s_3^* f_3^* - U_0|s_3^*|) \tag{37}$$

where $(f_1^*, f_2^*, f_3^*) = (D^{-1}F)^T$.

From (37), it is obvious that if the dc-link voltage U_0 satisfies

$$U_0 > \max_{i=1,2,3} |f_i^*| \tag{38}$$

then the time derivative of Lyapunov function dv/dt is negative definite and, hence, the origin in the space s^* is asymptotically stable. Note that since matrix D is nonsingular, sliding mode

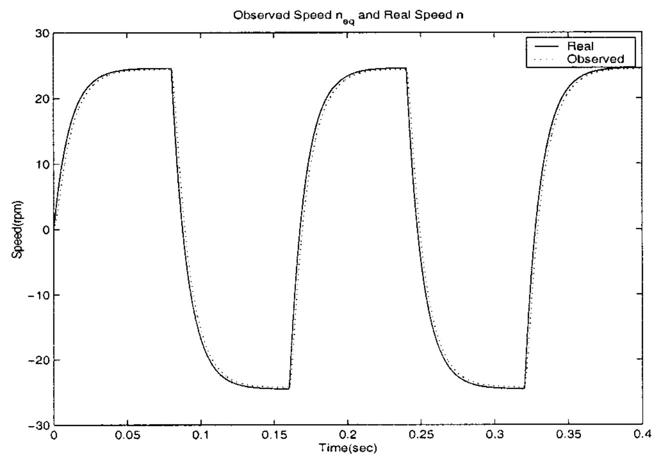

Fig. 4. Speed estimation.

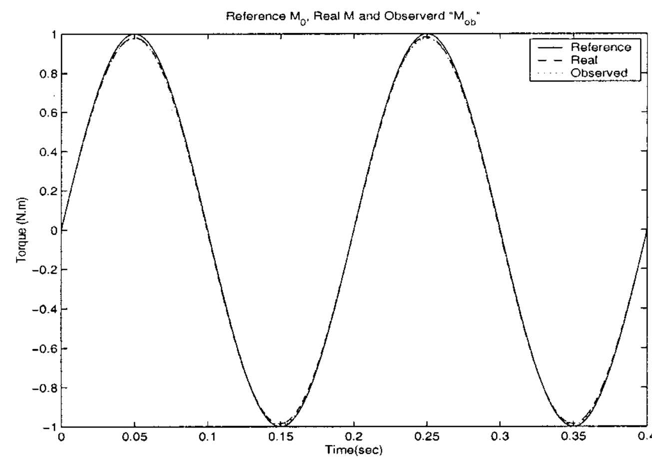

Fig. 6. Torque tracking.

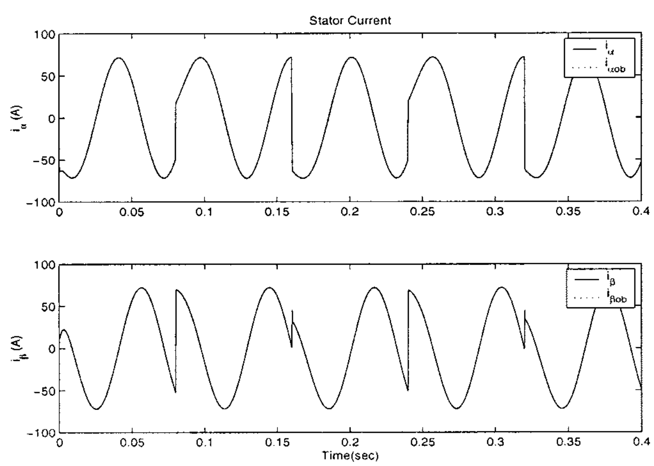

Fig. 5. Current convergence.

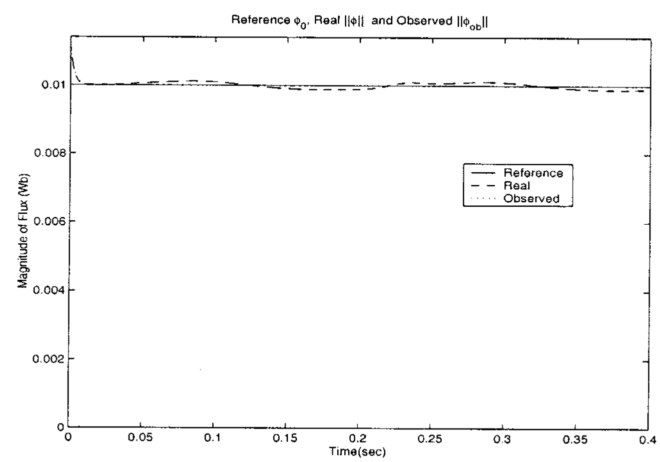

Fig. 7. Magnitude of flux tracking.

also arises in the manifold $s = 0$, which enables one to steer the estimated variables to the reference values.

VI. Composite Observer–Controller Analysis

As mentioned before, although the sliding-mode observer is of the fourth order, due to the order reduction of the sliding-mode equation, the error system of the observer is of the second order. To facilitate the analysis of the composite observer–controller tracking error system, we choose the errors e_1 and e_2 defined in (23) and (24) as the state variables of the error system.

Calculate the time derivative of the transformed flux errors e_1 and e_2 to build the error system of the rotor flux estimation

$$\dot{e}_1 = \dot{\overline{\phi}}_\alpha \hat{\phi}_\alpha + \dot{\overline{\phi}}_\beta \hat{\phi}_\beta + \overline{\phi}_\alpha \dot{\hat{\phi}}_\alpha + \overline{\phi}_\beta \dot{\hat{\phi}}_\beta \tag{39}$$

$$\dot{e}_2 = \dot{\overline{\phi}}_\beta \hat{\phi}_\alpha - \dot{\overline{\phi}}_\alpha \hat{\phi}_\beta + \overline{\phi}_\beta \dot{\hat{\phi}}_\alpha - \overline{\phi}_\alpha \dot{\hat{\phi}}_\beta \tag{40}$$

and find $\overline{\phi}_\alpha$ and $\overline{\phi}_\beta$ from (23) and (24),

$$\overline{\phi}_\alpha = \frac{\hat{\phi}_\alpha}{||\hat{\phi}||^2} e_1 - \frac{\hat{\phi}_\beta}{||\hat{\phi}||^2} e_2 \quad \overline{\phi}_\beta = \frac{\hat{\phi}_\beta}{||\hat{\phi}||^2} e_1 + \frac{\hat{\phi}_\alpha}{||\hat{\phi}||^2} e_2. \tag{41}$$

Substituting the right-hand sides of (9), (10), (15), (16), and the above two equations into (39) and (40) yields

$$\dot{e}_1 = \left(-2\eta + \eta \frac{x_H i_d}{||\hat{\phi}||}\right) e_1 + \eta \frac{x_H i_q}{||\hat{\phi}||} e_2 + \overline{n} e_2 - C\mu e_2 \tag{42}$$

$$\begin{aligned} \dot{e}_2 = &\left(-\eta + \eta \frac{x_H i_d}{||\hat{\phi}||}\right) e_2 - \left(n + \eta \frac{x_H i_q}{||\hat{\phi}||}\right) e_1 + \overline{n} e_1 \\ &- C||\hat{\phi}||^2 \mu + C\mu e_1 \end{aligned} \tag{43}$$

where

$$i_d = \frac{\hat{\phi}_\alpha}{||\hat{\phi}||} i_\alpha + \frac{\hat{\phi}_\beta}{||\hat{\phi}||} i_\beta \quad i_q = \frac{\hat{\phi}_\alpha}{||\hat{\phi}||} i_\beta - \frac{\hat{\phi}_\beta}{||\hat{\phi}||} i_\alpha. \tag{44}$$

i_d and i_q are the flux and torque components of the stator currents projected on the $(d,\, q)$ coordinate frame which is aligned with the estimates of the rotating field flux $\overline{n} = \hat{n} - n$. After sliding mode occurs, $\hat{n}$ should be replaced by $n_{\rm eq}$ in the motion equations. Therefore, the speed deviation $\overline{n}$ can be calculated from (27)

$$\overline{n} = -\frac{n}{||\hat{\phi}||^2} e_1 + \frac{\eta}{||\hat{\phi}||^2} e_2. \tag{45}$$

Substitution of (45) into (42) and (43) results in the error dynamics in matrix form

$$\begin{bmatrix}\dot e_1\\ \dot e_2\end{bmatrix}=\begin{bmatrix}-2\eta+\eta\dfrac{x_H i_d}{\|\hat\phi\|} & \eta\dfrac{x_H i_q}{\|\hat\phi\|}\\ -\left(n+\eta\dfrac{x_H i_q}{\|\hat\phi\|}\right) & -\eta+\eta\dfrac{x_H i_d}{\|\hat\phi\|}\end{bmatrix}\begin{bmatrix}e_1\\ e_2\end{bmatrix}+\begin{bmatrix}-C\mu e_2\\ -C\|\hat\phi\|^2\mu+C\mu e_1\end{bmatrix}+\begin{bmatrix}\dfrac{n}{\|\hat\phi\|^2}\,e_1e_2+\dfrac{\eta}{\|\hat\phi\|^2}\,e_2^2\\ \dfrac{n}{\|\hat\phi\|^2}\,e_1^2-\dfrac{\eta}{\|\hat\phi\|^2}\,e_1e_2\end{bmatrix}. \tag{46}$$

Assuming that sliding mode also arises on manifold $s_\mu=0$, and solving the algebraic equation $\dot s_\mu=0$ (26) with respect to μ,

$$\mu_{\text{eq}}=\frac{\eta}{\|\hat\phi\|^2}\,e_1+\frac{n}{\|\hat\phi\|^2}\,e_2 \tag{47}$$

we can eliminate the discontinuous parameter μ from the error system.

Since the estimates $\|\hat\phi\|$ and $\hat M$ track the reference inputs,

$$\phi_0=\|\hat\phi\| \tag{48}$$

$$\frac{d\|\hat\phi\|}{dt}=\frac{d\phi_0}{dt} \tag{49}$$

$$M_0=\frac{3P}{2}\,\frac{x_H}{x_R}(i_\beta\hat\phi_\alpha-i_\alpha\hat\phi_\beta). \tag{50}$$

To express (9), (49), and (50) in the d–q frame, find i_α, i_β from (44)

$$i_\alpha=\frac{\hat\phi_\alpha}{\|\hat\phi\|}\,i_d-\frac{\hat\phi_\beta}{\|\hat\phi\|}\,i_q,\quad i_\beta=\frac{\hat\phi_\alpha}{\|\hat\phi\|}\,i_q+\frac{\hat\phi_\beta}{\|\hat\phi\|}\,i_d. \tag{51}$$

For constant ϕ_0, after substituting the above two equations and (9), (10), and (48) into (49) and (50), we have

$$i_q=\frac{2x_R M_0}{3Px_H\phi_0} \tag{52}$$

$$-\eta+\eta x_H\,\frac{i_d}{\|\hat\phi\|}=0. \tag{53}$$

Finally, substituting (47), (48), (52), and i_d from (53) into the error dynamic system (46), and performing linearization, we get

$$\begin{bmatrix}\dot e_1\\ \dot e_2\end{bmatrix}=\begin{bmatrix}-\eta & a\\ -(n_{\text{eq}}+a)-C\eta & -Cn_{\text{eq}}\end{bmatrix}\begin{bmatrix}e_1\\ e_2\end{bmatrix} \tag{54}$$

where $a=(2M_0r_R/3P\phi_0^2)$.

Note that the linearized error system does not depend on the real speed, real rotor flux, and real stator current. It depends only on the reference torque, the magnitude of the reference flux, the equivalent angle speed, and the adjustable parameter C. As follows from (54), for large C, the motion of the error dynamic system can be decomposed into the slow and fast motion [14]. The fast component $\eta e_1+n_{\text{eq}}e_2$ decays rapidly with

$$\lim_{t\to\infty}e_2=-\frac{\eta}{n_{\text{eq}}}\,e_1. \tag{55}$$

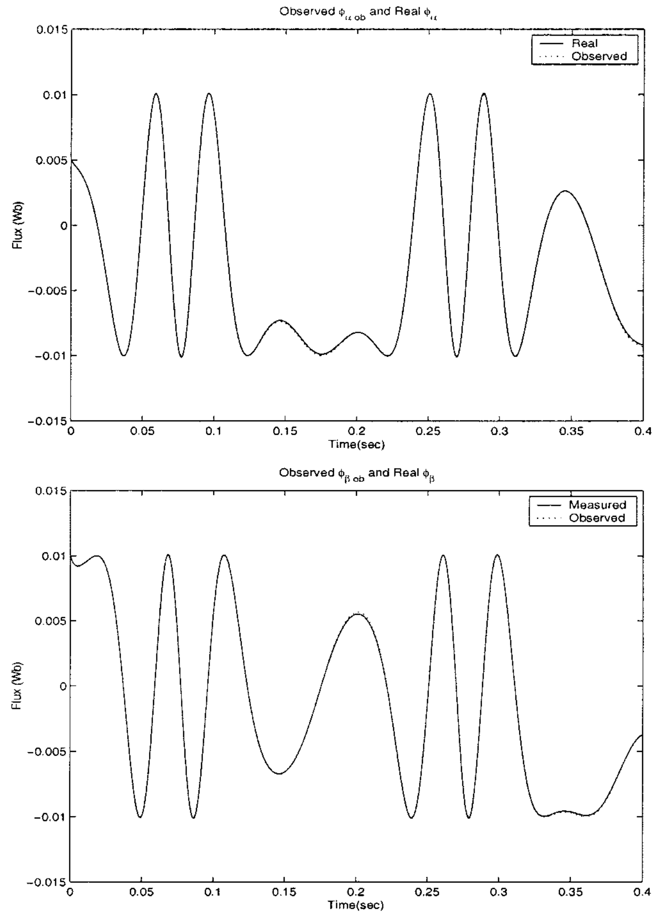

Fig. 8. Flux convergence.

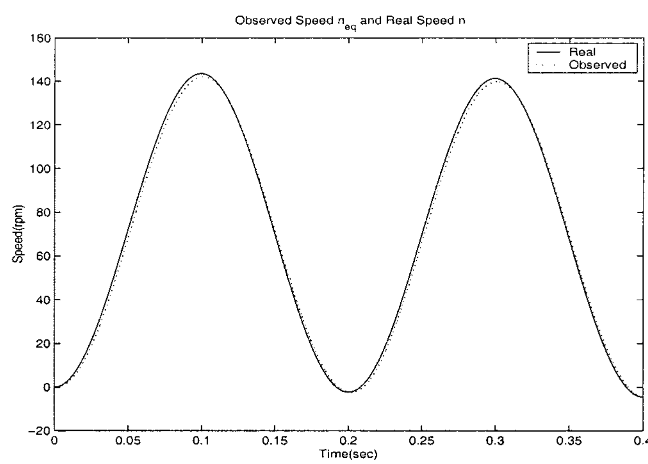

Fig. 9. Speed estimation.

The slow motion is governed by

$$\dot e_1=-\eta\left(1+\frac{a}{n_{\text{eq}}}\right)e_1. \tag{56}$$

One of the sufficient conditions for the asymptotic stability of the slow motion for any time-varying speed is $1+(a/n_{\text{eq}})>0$. It is clear that

$$\frac{a}{n_{\text{eq}}}>0 \tag{57}$$

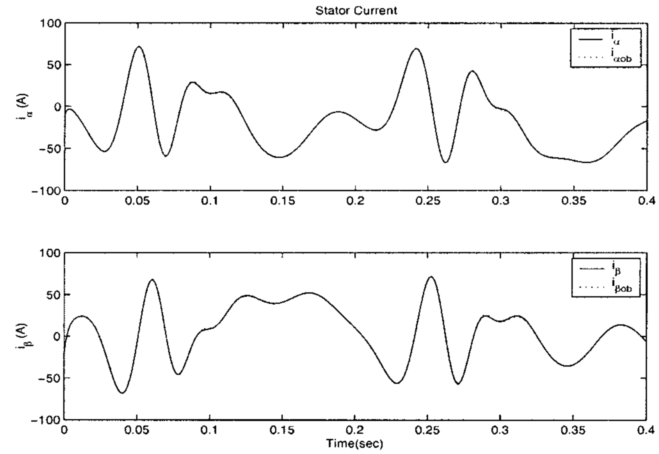

Fig. 10. Current convergence.

is a sufficient condition as well. It means that the solution to (56) is stable and $\lim_{t\to\infty} e_1 = 0$ if the reference torque and the equivalent speed have the same sign. We have described qualitatively the design procedure based on motion separation approach. The details may be found in [14]. According to (55), $\lim_{t\to\infty} e_2 = 0$.

Remark 4: According to [14], the asymptotic stability of the fast motion of the error dynamic (54) requires that the parameter C and $n_{\rm eq}$ have the same sign. Since the equivalent speed can be calculated through equation (28) online, the sign of the parameter C can be adapted to the sign of the equivalent speed. At the instants when $n_{\rm eq} = 0$, according to (57), the sign of parameter C can be adapted to the sign of the reference torque, and then the stability of the system can also be guaranteed.

Remark 5: The proposed torque regulation is insensitive to the variation of the load torque. Even the sign of the load torque will not affect the stability of the observer–controller.

VII. Simulation Results

The proposed control scheme was first simulated using MATLAB. In the simulation, pulsewidth modulation (PWM) technique is not used and the dynamics in the voltage-source inverter are also ignored. In [2], this control approach is called direct control.

One point that should be noted is the calculation of the derivative of the rotor flux amplitude $d\|\hat{\phi}\|/dt$. To avoid too much noise, it is not desirable to differentiate directly to obtain the time derivative of $\|\hat{\phi}\|$ and, even though $d\phi_\alpha/dt$ and $d\phi_\beta/dt$ are discontinuous functions, the derivative $d\|\hat{\phi}\|/dt$ should be a continuous function of time t, otherwise the sliding surface s_2 would be a discontinuous function, and sliding mode cannot be enforced in such a manifold. Note that $(d\|\hat{\phi}\|/dt) = (\hat{\phi}_\alpha/|\hat{\phi}|)(d\hat{\phi}_\alpha/dt) + (\hat{\phi}_\beta/|\hat{\phi}|)(d\hat{\phi}_\beta/dt)$. It can be seen that the discontinuity introduced by the discontinuous parameter μ is cancelled. We can eliminate another discontinuous parameter $\hat{n}$ by replacing $\hat{n}$ by $n_{\rm eq}$ which is continuous. This will not destroy the sliding mode because sliding mode is enforced through the stator current.

Parameters used in the torque controller, in the flux/speed observer, and of the IM model for the simulation are listed in Table I. Figs. 1–10 show the simulation results. Figs. 1–5 show the piecewise continuous situation, while Figs. 6–10 show the sinusoidal situation for the torque tracking. From these simulation results, we can see that the proposed sliding-mode speed/flux observer exhibits high accuracy. Note that convergence of estimations to real values of flux and speed takes place if torque estimate tracks the reference input. This condition cannot be fulfilled for piecewise continuous input and discontinuities result in converging transient processes. This phenomenon may be observed in the simulation.

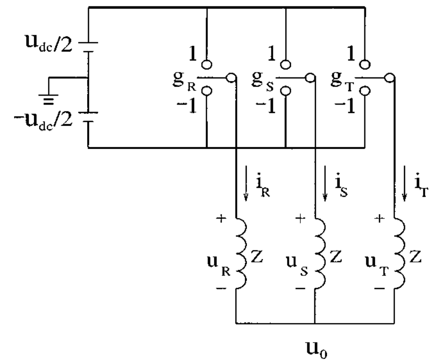

Fig. 11. PWM implementation.

VIII. Implementation Issues

A. Sliding-Mode Control Scheme in Terms of Phase Voltages $u_i (i = R, S, T)$

In this section, it will be shown that we can use sliding-mode method for direct control of a converter.

Fig. 11 shows the system configuration for the PWM implementation. There are three control signals g_R, g_S, and g_T, which control the on–off switches in the three phases. We only assign $+1$ or -1 to these three signals, which correspond to voltage value $(u_{dc}/2)$ or $-(u_{dc}/2)$ (with respect to ground level). From the circuit analysis, the following circuit equations for the three phases are obtained:

$$\begin{cases} i_R \cdot Z = u_R = g_R \cdot \dfrac{u_{dc}}{2} - u_0 \\ i_S \cdot Z = u_S = g_S \cdot \dfrac{u_{dc}}{2} - u_0 \\ i_T \cdot Z = u_T = g_T \cdot \dfrac{u_{dc}}{2} - u_0. \end{cases}$$

From the physical configuration of the circuit, we know the sum of the left sides is equal to zero, which gives us: $0 = (g_R + g_S + g_T)(u_{dc}/2) - 3u_0$. Then, the voltage of the central point is obtained $u_0 = (1/3)(\sum_{i=R,S,T} g_i)(u_{dc}/2)$, from which the phase voltage is obtained: $u_i = g_i(u_{dc}/2) - (1/3)(\sum_{i=R,S,T} g_i)(u_{dc}/2)$ with $i = R, S, T$. Therefore,

$$\begin{bmatrix} u_R \\ u_S \\ u_T \end{bmatrix} = \frac{1}{3}\Gamma \begin{bmatrix} g_R \\ g_S \\ g_T \end{bmatrix} \frac{u_{dc}}{2} \quad \text{with} \quad \Gamma = \begin{bmatrix} 2 & -1 & -1 \\ -1 & 2 & -1 \\ -1 & -1 & 2 \end{bmatrix}. \tag{58}$$

Note that, for any control commands u_i, the balance condition $\sum_{i=R,S,T} u_i = 0$ holds and we may implement three

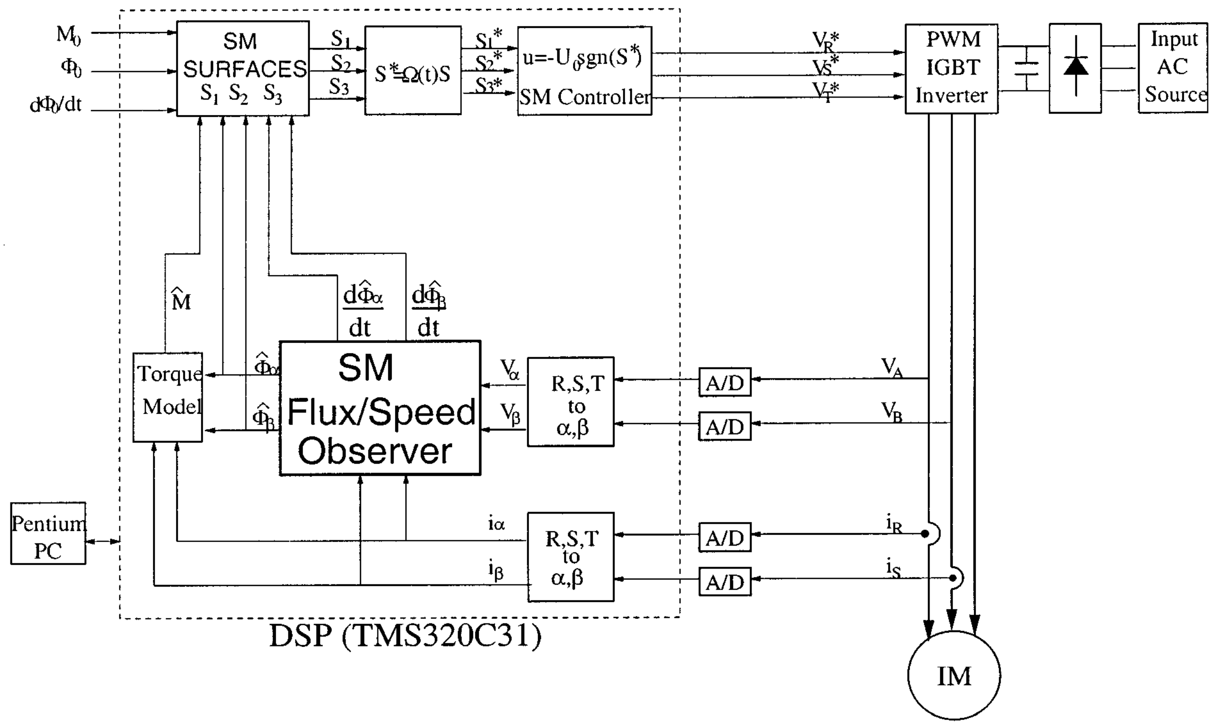

Fig. 12. System block diagram.

TABLE II
REAL INDUCTION MOTOR DATA

5 Hp	$r_S = 0.6\Omega$
220 v	$r_R = 0.412\Omega$
14.8 A	$x_S = 0.0431H$
60 Hz	$x_R = 0.0431H$
1720 rpm	$x_H = 0.0412H$

TABLE III
BASE SYSTEM DATA

$V_b = 500V$	$I_b = 50A$
$R_b = 10\Omega$	$f_b = 100Hz$
$\omega_b = 2\pi f_b$	$\phi_b = V_b/\omega_b$
$M_b = 1.5PI_b\phi_b$	

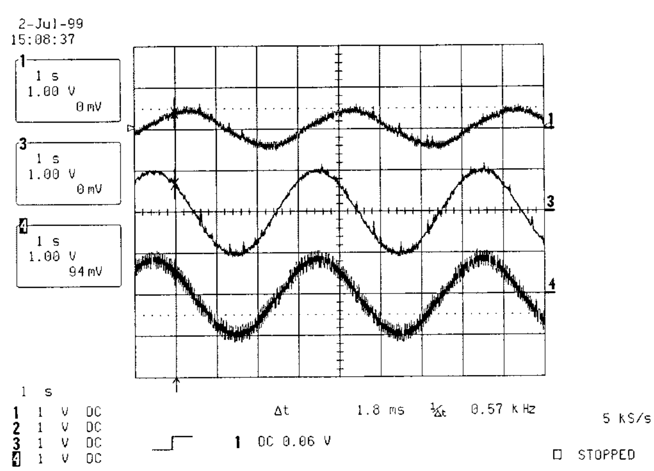

Fig. 13. Torque control with speed sensor. Curve 1: $n_{\rm real}$; curve 3: $M_{\rm ref} * 10$ (amplitude: 0.01 $M_b = 1.19$ N·m); curve 4: $M_{\rm real} * 10$.

phase voltages $f_R(t)$, $f_S(t)$, and $f_T(t)$ only if they satisfy $\sum_{i=R,S,T} f_i = 0$. The PWM implementation algorithm is designed as follows:

$$\dot{z}_i = f_i - U_0\,\mathrm{sign}(z_i), \qquad i = R, S, T.$$

It is clear that, if scalar U_0 is large enough, sliding mode occurs on the surfaces $z_i = 0$. Using equivalent control concepts, we know that $[U_0\,\mathrm{sign}(z_i)]_{\rm eq} = f_i$.

After assigning $g_i = \mathrm{sign}(z_i)$ and substituting them into voltage equation, we get

$$\begin{bmatrix} u_R \\ u_S \\ u_T \end{bmatrix} = \frac{u_{dc}}{6}\Gamma \begin{bmatrix} \mathrm{sign}\, z_R \\ \mathrm{sign}\, z_S \\ \mathrm{sign}\, z_T \end{bmatrix}.$$

In sliding mode, the motion equations become

$$\begin{aligned} \begin{bmatrix} u_R \\ u_S \\ u_T \end{bmatrix}_{\rm eq} &= \frac{u_{dc}}{6}\Gamma \begin{bmatrix} \mathrm{sign}\, z_R \\ \mathrm{sign}\, z_S \\ \mathrm{sign}\, z_T \end{bmatrix}_{\rm eq} = \frac{u_{dc}}{6U_0}\Gamma \begin{bmatrix} f_R \\ f_S \\ f_T \end{bmatrix} \\ &= \frac{u_{dc}}{6U_0} \begin{bmatrix} 2f_R - f_S - f_T \\ 2f_S - f_R - f_T \\ 2f_T - f_R - f_S \end{bmatrix} = \frac{u_{dc}}{2U_0} \begin{bmatrix} f_R \\ f_S \\ f_T \end{bmatrix}. \end{aligned}$$

If $u_{dc} = 2U_0$, then $(u_i)_{\rm eq} = f_i$, which shows that this algorithm provides a feasible scheme for PWM implementation.

For the voltage equation (58), we have the following observations.

1) There are altogether eight situations for the on–off states of the three switches g_R, g_S, and g_T. For the situations in which all $g_i = 1$ or $g_i = -1$, each phase voltage $u_i = 0$.

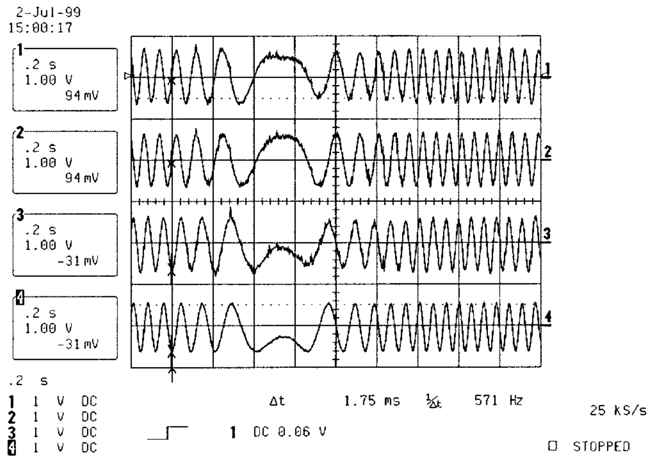

Fig. 14. Flux estimation. Curves 1 and 3: $\hat{\phi}_\alpha$ and $\hat{\phi}_\beta$ from observer with sensor. Curves 2 and 4: $\hat{\phi}_\alpha$ and $\hat{\phi}_\beta$ from SM observer without sensor.

2) For the other six situations, the magnitude of one phase voltage is $(4/3)|(u_{dc}/2)|$, while the magnitude of the other two is $(2/3)|(u_{dc}/2)|$.

Obviously, all eight combinations satisfy the balance condition, although it never holds for g_i.

B. Sliding-Mode Control Scheme in Terms of g_i with $i = R, S, T$

In this section, it is shown that sliding-mode control can be implemented in terms of g_i directly instead of u_i. We design the sliding surfaces as

$$s_1 = M_0 - M$$
$$s_2 = c_2(\phi_0 - \|\phi\|) + \frac{d}{dt}(\phi_0 - \|\phi\|)$$
$$s_3 = \int_0^t (g_R + g_S + g_T)\, dt.$$

After sliding mode occurs, $(g_R + g_S + g_T)_{\mathrm{eq}} = 0$, then

$$\begin{bmatrix} u_R \\ u_S \\ u_T \end{bmatrix}_{\mathrm{eq}} = \frac{u_{dc}}{6}\Gamma \begin{bmatrix} g_R \\ g_S \\ g_T \end{bmatrix}_{\mathrm{eq}} = \frac{u_{dc}}{2} \begin{bmatrix} g_R \\ g_S \\ g_T \end{bmatrix}_{\mathrm{eq}}.$$

This means $(u_i)_{\mathrm{eq}} = k(g_i)_{\mathrm{eq}}$. Therefore, the voltage balance condition can be satisfied automatically, i.e., $(u_R + u_S + u_T)_{\mathrm{eq}} = 0$. From here, it is concluded that if one of the sliding surfaces is designed as the balance condition for g_i, we can design the control in terms of g_i. In other words, g_i can be handled as phase voltages.

We can also design two-dimensional sliding mode in terms of the three switches command g_i. In this case, there are only two sliding-mode surfaces

$$s_1 = M_0 - M$$
$$s_2 = c_2(\phi_0 - \|\phi\|) + \frac{d}{dt}(\phi_0 - \|\phi\|)$$
$$\begin{bmatrix} \dot{s}_1 \\ \dot{s}_2 \end{bmatrix} = \begin{bmatrix} f_1 \\ f_2 \end{bmatrix} + D \begin{bmatrix} u_R \\ u_S \\ u_T \end{bmatrix} = F + \frac{u_{dc}}{6} D\Gamma \begin{bmatrix} g_R \\ g_S \\ g_T \end{bmatrix} = F + D\Gamma G$$

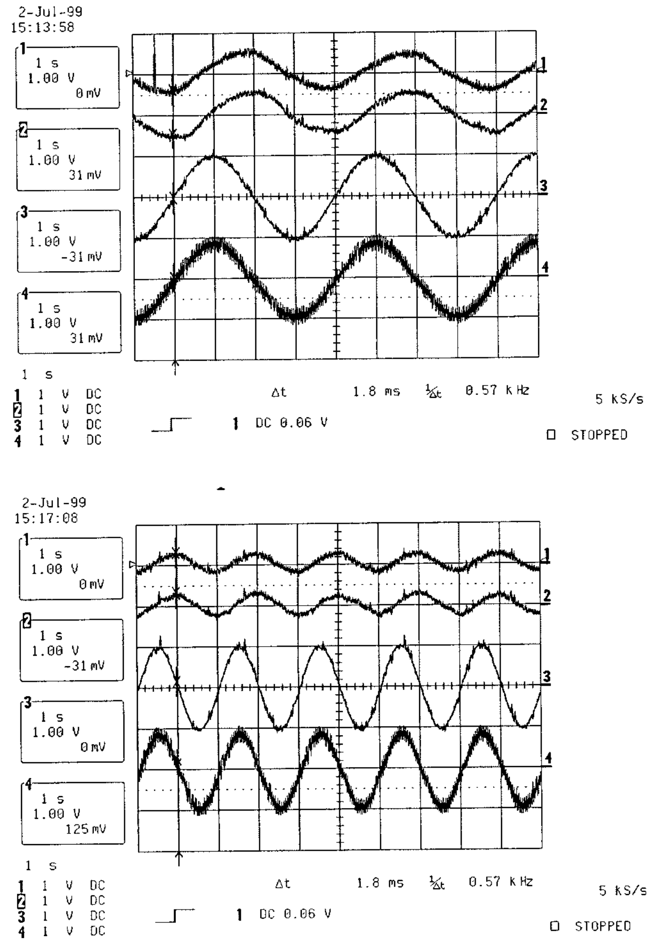

Fig. 15. Sensorless torque control. Curve 1: n_{real} from sensor; curve 2: n_{eq} from observer; curve 3; $M_{\mathrm{ref}} * 10$; curve 4: $\hat{M}_{real} * 10$. Top: case 1 (period time is 4 s); bottom: case2 (period time is 2 s).

where

$$D = \begin{bmatrix} \frac{2}{3}a_1(e_R \times \phi) & \frac{2}{3}a_1(e_S \times \phi) & \frac{2}{3}a_1(e_T \times \phi) \\ \frac{2}{3}a_2(e_R \cdot \phi) & \frac{2}{3}a_2(e_S \cdot \phi) & \frac{2}{3}a_2(e_T \cdot \phi) \end{bmatrix}$$

and

$$G = \frac{u_{dc}}{6}\begin{bmatrix} g_R \\ g_S \\ g_T \end{bmatrix}.$$

Choose the Lyapunov function as $V = (1/2)s^T s$, then $\dot{V} = s^T \dot{s} = s^T F + s^T D\Gamma G$. Let $(s^*)^T = s^T(D\Gamma)$, then $(s^*)^T(D\Gamma)^{-1} = s^T$. Note that $(D\Gamma)^{-1}$ denotes the pseudo-inverse of $(D\Gamma)$, which is a 3×2 matrix. Since $\dot{V} = s^T F + (s^*)^T G$, implement the three PWM switches by the command $g_i = -\mathrm{sign}\, s_i^*$, i.e., $G = -U_o\, \mathrm{sign}\, s^*$. Then, $\dot{V} = (s^*)^T(D\Gamma)^{-1}F - U_0(s^*)^T \mathrm{sign}\, s^* \leq \|(s^*)^T\|\|(D\Gamma)^{-1}\|\|F\| - U_0\|s^*\|$. If $U_0 \geq \|(s^*)^T\|\|F\|$, $\dot{V} \leq 0$ so that sliding mode can occur.

IX. Experiment Setup and Results

The proposed control scheme was also implemented in the laboratory. The real-time control and estimation program was written in C language.

The proposed algorithm was tested at the experiment environment in the Power Electronics and Electrical Machines (PEEM) Laboratory, The Ohio State University, Columbus. The motor is a Westinghouse 5-hp 220-V Y-connected four-pole induction machine with the parameters listed in Table II. The block diagram of the torque control system is shown in Fig. 12. The part within the dashed line is implemented by a digital signal processor (DSP) system. Instead of the fixed-point DSP system, we used a PC plug-in DS1102 dSpace system, which includes TMS320C31 32-bit floating-point DSP as the main processing unit and a set of on-board peripherals frequently used in digital control systems.

The main components of the experiment environment include the following: a DSP system; an IM and associated voltage-source inverters; an optical encoder attached to the motor shaft for speed estimation verification and comparison; cables for connecting the whole analog/digital signals; and ac current sensors.

The torque control is executed every 100 μs, which gives a switching frequency of the insulated gate bipolar transistor (IGBT) inverter at around 12.5 kHz. Since the system was tested with no load, we had to apply a sign-varying torque reference input.

To verify and compare the estimated flux of our sliding-mode observer, a reduced-ordered observer is designed with the state vector $(\hat{\phi}_\alpha, \hat{\phi}_\beta)$ as the estimate of rotor flux components. In this observer, the required information is stator current i_α, i_β and the rotor speed n, which are obtained from the sensor and encoder, respectively. The observer model is as follows:

$$\frac{d\hat{\phi}_\alpha}{dt} = -\eta\hat{\phi}_\alpha - n\hat{\phi}_\beta + \eta x_H i_\alpha$$
$$\frac{d\hat{\phi}_\beta}{dt} = -\eta\hat{\phi}_\beta + n\hat{\phi}_\alpha + \eta x_H i_\beta.$$

It is easily proven that this observer guarantees the exponential convergence of the estimated stator flux to the real flux [1].

All the experiments are conducted in the so-called per-unit system, whose base parameters are listed in Table III. All the experimental results obtained are expressed in the per-unit system.

Fig. 13 shows the result of the experiment in which only the sliding-mode controller is implemented while the speed is from the optical sensor. $\hat{M}_{real}$ is defined as follows: $\hat{M}_{real} = (3P/2)(x_H/x_R)(i_\beta\hat{\phi}_\alpha - i_\alpha\hat{\phi}_\beta)$. The flux is from the above reduced-ordered observer. Fig. 14 shows the flux estimations of our fourth-order sliding-mode observer. We also compare them with the flux estimation from the reduced-ordered observer. Fig. 15 shows the results for the system with both the sliding-mode controller and sliding-mode observer working. In this case, we do not need to use the optical sensor to obtain the speed, i.e., sensorless control. All the variables needed for torque or speed control, such as flux components, their derivatives, and speed, are obtained from the sliding-mode observer.

Speed control can also be achieved through torque control. In our experiments, with zero load, $(dn/dt) = (P/J)M$. As shown above, the estimate $n_{\rm eq}$ tends to n, therefore, if the torque is set as $k(n_{\rm eq} - n_0)$, then $(dn/dt) = (kP/J)(n_{\rm eq} - n_0)$ and the motor speed converges to n_0 exponentially with the rate decided by the parameter (kJ/P). Figs. 16 and 17 show the results for speed control. Fig. 16 shows the case in which the speed is

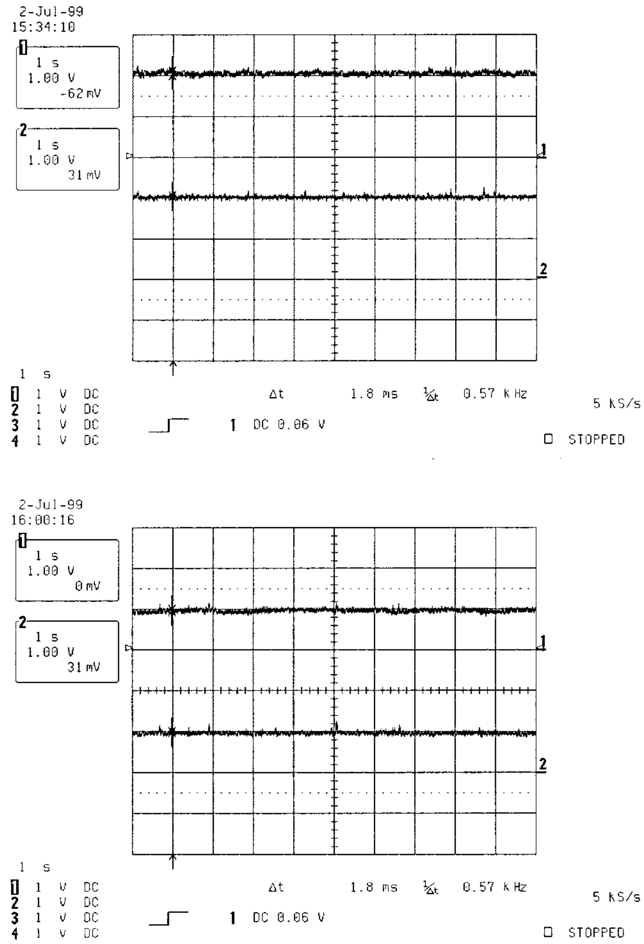

Fig. 16. Sensorless speed control. Curve 1: $n_{\rm real}$; curve 2: $n_{\rm eq}$. Top: case 1, $n_{\rm ref} = 0.2$ (600 r/min); bottom: case 2, $n_{\rm ref} = 0.1$ (300 r/min).

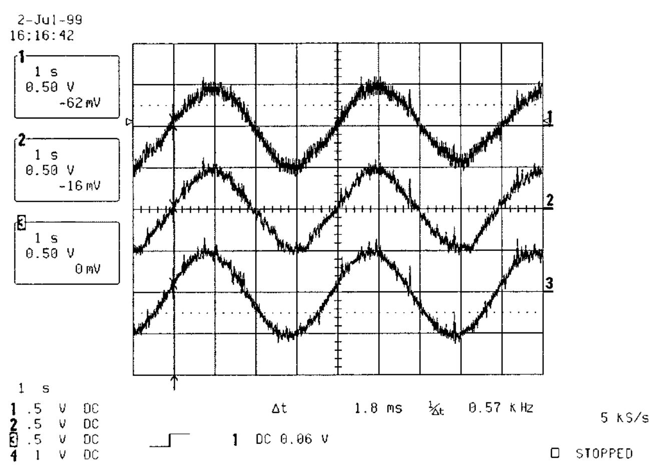

Fig. 17. Sensorless speed control. Curve 1: $n_{\rm real}$; curve 2: $n_{\rm eq}$; curve 3: $n_{\rm ref}$. Case 3: $N_{\rm ref} = 0.05\sin[(\pi/2)t]$.

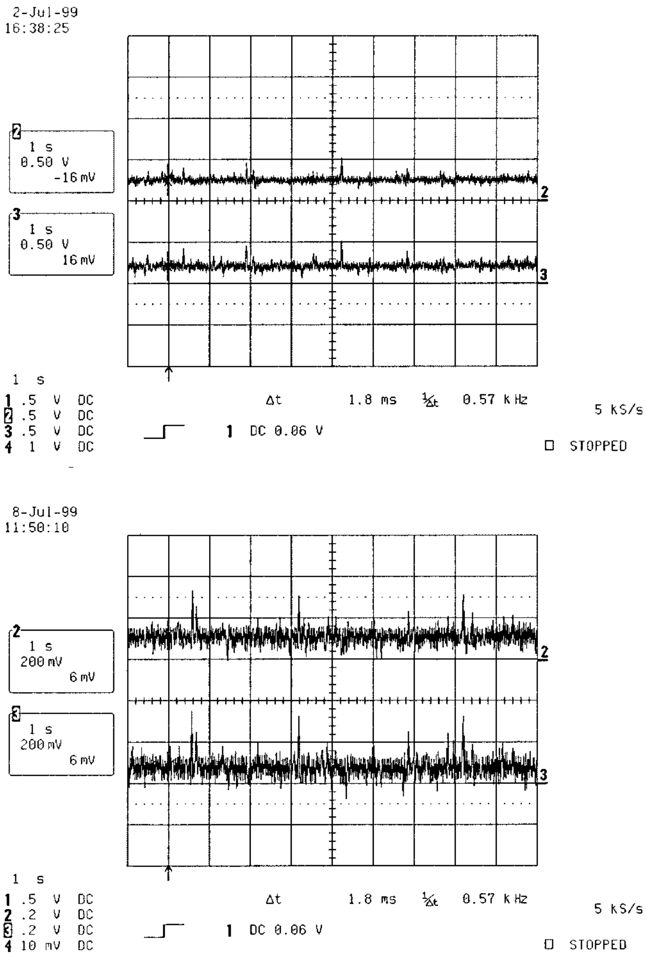

Fig. 18. Low-speed control. Curve 2: $20 * n_{\rm real}$; curve 3: $20 * n_{\rm eq}$. Top: case1, $n_{\rm ref} = 0.00125$ (3.75 r/min); bottom: case 2, $n_{\rm ref} = 0.0005$ (1.5 r/min)

constant, while Fig. 17 shows the case with time-varying speed reference input.

X. SLIDING-MODE CONTROLLER IN LOW-SPEED SITUATION

Currently, low-speed control is still a challenging issue for IMs. The potential of sliding-mode control and estimation methodology was tested experimentally for the low-speed case with the speed measurement. We still use the speed control method discussed above, but the speed information is obtained from the sensor. The results are shown in Fig. 18. We can see that, even for very low speed (1.5 r/min), the controller demonstrates good performance.

XI. CONCLUSIONS

In this paper, a new sliding-mode observer/controller algorithm has been developed for the estimation of the rotor flux and the angle speed and the torque control of an IM without measurement of any mechanical variables, such as speed and torque. Error analysis of the observer has been performed, which shows that, for any time-varying angle speed, the asymptotic stability of the observer can be achieved. We also implemented the system using a DSP and showed its performance through laboratory experiments. The experiments show that the proposed sliding-mode controller/observer works well for a wide speed range, and the controller itself is very promising for a low-speed situation. Sliding-mode approach may be considered in the view of the field-oriented concept, which implies coordinate transformation provides decoupling of flux and torque (speed) control loops. Exact decoupling is feasible if complete information on system states and parameters is available. Sliding-mode approach exhibits a robustness property with respect to coordinate transformation, because after sliding mode occurs, exact decoupling takes place even if both the dynamics are interconnected before it starts.

REFERENCES

[1] V. I. Utkin, "Sliding mode control design principles and applications to electric drives," *IEEE Trans. Ind. Electron.*, vol. 40, pp. 23–36, Feb. 1993.
[2] B. K. Bose and M. G. Simoes, "Speed sensorless hybrid vector controlled induction motor drive," in *Conf. Rec. IEEE-IAS Annu. Meeting*, 1995, pp. 137–143.
[3] K. M. H. Kubota and T. Nakano, "DSP-based speed adaptive flux observer of induction motor," *IEEE Trans. Ind. Applicat.*, vol. 29, pp. 344–348, Mar./Apr. 1993.
[4] C. Schauder, "Adaptive speed identification for vector control of induction motors without rotational transducers," in *Conf. Rec. IEEE-IAS Annu. Meeting*, 1989, pp. 493–499.
[5] H. Tajima and Y. Hori, "Speed sensorless field oriented control of induction motor," *IEEE Trans. Ind. Applicat.*, vol. 29, pp. 175–180, Jan./Feb. 1993.
[6] J. W. Dixon and J. N. Rivarola, "Induction motor speed estimator and synchronous motor position estimator based on a fixed carrier frequency signal," *IEEE Trans. Ind. Electron.*, vol. 43, pp. 505–509, Aug. 1996.
[7] H.-W. Kim and S.-K. Sul, "A new motor speed estimator using Kalman filter in low-speed range," *IEEE Trans. Ind. Electron.*, vol. 43, pp. 498–504, Aug. 1996.
[8] V. I. Utkin, J. Guldner, and J. Shi, *Sliding Mode Control in Electromechanical Systems*. New York: Taylor & Francis, 1999.
[9] A. Zaremba, "Reduced order sliding mode speed observer of induction motors," Ford Company, Dearborn, MI, Tech. Rep., 1995.
[10] D. Izosimov, "Multivariable nonlinear induction motor state identifier using sliding modes" (in Russian), in *Problems of Multivariable Systems Control*. Moscow, U.S.S.R.: Nauka, 1983.
[11] V. I. Utkin, *Sliding Modes in Control and Optimization*. Berlin, Germany: Springer-Verlag, 1992.
[12] W. Leonard, *Control of Electrical Drives*. Berlin, Germany: Springer-Verlag, 1985.
[13] D. W. Novotny and T. A. Lipo, *Vector Control and Dynamics of AC Drives*. London, U.K.: Oxford Univ. Press, 1996.
[14] P. Kokotovic, H. K. Khalil, and J. O'Reilly, *Singular Perturbation Methods in Control: Analysis and Design*. New York: Academic, 1986.

Zhang Yan was born in Nanjing, China. He received the B.S. degree in electrical engineering in 1995 from Southeast University, Nanjing, China, and the M.S. degree in electrical engineering in 1999 from The Ohio State University, Columbus, where he is currently working toward the Ph.D. degree in the Department of Electrical Engineering.

His research interests include sliding-mode control and electrical machine drives.

Changxi Jin was born in Zhejiang, China, in 1969. He received the B.E. degree from Harbin Institute of Technology, Harbin, China, and the M.S degree from The Ohio State University, Columbus, OH, in 1991 and 1997, respectively, both in electrical engineering.

In 1997, he joined Fujitsu USA, Santa Clara, CA, as a Design Engineer. Since then, he has been involved in microprocessor and computer peripheral devices design and verification and embedded system design.

Vadim I. Utkin (SM'96) received the Dipl. Eng. degree from Moscow Power Institute, Moscow, Russia, and the Ph.D. degree from the Institute of Control Sciences, Moscow, Russia.

He joined the Institute of Control Sciences in 1960 and was Head of the Discontinuous Control Systems Laboratory from 1973 to 1994. He is currently Ford Chair of Electromechanical Systems at The Ohio State University, Columbus. He has held visiting positions at universities in the U.S., Japan, Italy, and Germany. He is one of the originators of the concepts of variable-structure systems and sliding-mode control. He is the author of five books and more than 250 technical papers. His current research interests are control of infinite-dimensional plants, including flexible manipulators, sliding modes in discrete-time systems, and microprocessor implementation of sliding-mode control, control of electric drives, alternators and combustion engines, robotics, and motion control. He was IPC Chairman of the 1990 IFAC Congress in Tallinn, U.S.S.R. He is currently an Associate Editor of the *International Journal of Control*.

Dr. Utkin is an Honorary Doctor of the University of Sarajevo, Yugoslavia. In 1972, he was awarded the Lenin Prize (the highest scientific award in the former U.S.S.R.).